Research Article

Application of Linear Additive Conditions for Near-Infrared Diffuse Reflectance Absorption Spectroscopy

Zhiyue Feng [iD],[1] Guimin Cai [iD],[2] Tiancheng Huang [iD],[1] Hubin Liu [iD],[1] Jianhua Zheng [iD],[1] Zengrong Yang [iD],[1] Longlian Zhao [iD],[1] and Junhui Li [iD][1]

[1]*College of Information and Electrical Engineering, China Agricultural University, Beijing, China*
[2]*Shanghai Lengguang Technology, Shanghai, China*

Correspondence should be addressed to Junhui Li; caunir@cau.edu.cn

Determining the homogeneity of material mixing in real time during product processing is critical for quality control. According to the Kubelka–Munk (K-M) function of diffuse reflectance absorption spectrum, absorbance (A) is approximately linear with the content of the components when the sample scattering coefficient (S) is in a certain range. The S is determined by the particle size of powder samples. Therefore, this study determined particle size ranges that satisfy linear additivity in near-infrared diffuse reflectance spectroscopy (NIRDRS). Thus, the proposed NIRDRS analysis technique can be used to determine the homogeneity of material mixes or analyze the percentages of the components in the mixture. In this study, vitamin B3 and vitamin C were used for preparing mixed samples with varying percentages. The experimental results revealed that linear additivity is satisfied when the powder particle size is in the range of less than 280, 280–450, and 450–900 μm. When the confidence level is 0.01, the actual mixed spectra are not significantly different from the "simulated mixed spectra" constructed by linear addition, with their relative deviations less than 1.08%. The absolute errors of the actual and analytic percentages were within 2.98% for each component in the mixtures. The above conclusions also hold for sorghum, which has a complex material composition. Statistical models cannot analyze the percentages of components in the mixture. In contrast, linear addition and direct calibration approach avoids the use of a large number of samples for statistical modeling and analyze the percentages of mixed samples. Meanwhile, it can be used to discriminate and analyze the material mixing uniformity by building a mechanistic model.

1. Introduction

Near-infrared (NIR) diffuse reflectance spectroscopy can provide rapid analysis and the simultaneous determination of multiple components, and it does not require chemical reagents. Considerable progress has been made in using this technique in the quality and safety evaluation of medicine, as well as food and feed [1–5]. Medicine and agricultural products are high-value commodities that considerably affect people's lives. The formulation design and mixing uniformity of the products are critical indicators for evaluating their quality. If the mixture is not uniform, the percentage and effectiveness of the product is severely affected. Vitamin B3 and vitamin C are the essential nutrients for maintaining the normal functions and metabolic activities of the body [6–9]. The homogeneity of the drug powder mixture considerably influences the consistency and stability of medicine quality. Testing is required to determine whether the actual content is consistent with the labeled content. Sorghum is used in brewing, food processing, and breeding [10–12]. However, japonica and glutinous sorghum are used for different purposes. Raw material proportioning and mixing uniformity in processing and production considerably affect product utilization and nutritional value.

Image analysis [13–15], UV-visible absorption spectrophotometry [16–21], and high-performance liquid chromatography (HPLC) [22–26] are typically used for determining mixing uniformity. The image analysis method requires particles of various colors and distinguishing between components of similar colors. UV and HPLC methods

require a laboratory environment, which increases the difficulty and cost of detection. Determining the mixing uniformity method requires the establishment of predictive models in conventional quantitative NIR spectroscopy techniques. The accuracy of the technique depends on the established quantitative model. Furthermore, model maintenance and update become complex at a subsequent stage [27–29]. Therefore, the development of a rapid and accurate quality monitoring and detecting method is critical for ensuring the uniform mixing of agricultural products and medicine.

Yan et al. [30] verified the additivity of NIR diffuse reflectance spectra and stated that for transmission spectroscopy, the absorbance (A) and the component content are proportionally linear according to Beer's law. Therefore, transmission spectrum exhibits the additivity of spectral absorbance because diffuse reflectance spectroscopy can be converted based on the K-M function. A and K/S can be approximated by a straight line with intercept not equal to zero when the sample concentration range is small and S is within a certain range. Thus, K is proportional to the component content, such that A is approximately linear with the component content. Therefore, the diffuse reflectance spectrum of the solid exhibits a linear additive property.

This study combined the linear additivity of NIR diffuse reflectance with the formulation regression algorithm. The particle size range satisfying the linear additivity was verified experimentally. Furthermore, a method to determine the homogeneity of a mixture was proposed. Comparing the absolute error between the analytic and actual percentages or the difference between the simulated mixture homogeneity spectrum and the actual mixture spectrum can reveal the homogeneity status of the mixture. This technique is a low-cost determination method that does not require statistical modeling of multiple samples.

2. Materials and Methods

2.1. Material

(i) Starch-containing vitamin (vitamin B3 and vitamin C) tablets were procured from Tianjin Lisheng Pharmaceutical Co., Ltd. In this experiment, five particle size ranges of $>900\,\mu m$, $450–900\,\mu m$, $280–450\,\mu m$, $180–280\,\mu m$, and $<180\,\mu m$ were obtained by grinding and sieving. All the mixed samples were prepared according to the mass percentage of 50%–50%. The particle sizes of the samples in the mixture are presented in Table 1:

(ii) In this experiment, glutinous sorghum obtained from Shandong, China, Yungu sorghum and japonica sorghum obtained from Liaoning, China, and Farmer sorghum were used as raw materials. Raw powder material was obtained by grinding and sieving from 280 to $450\,\mu m$. Five groups of mixture test samples were prepared as presented in Table 2.

2.2. Instruments and Measurement Methods. The preparation process of the mixed samples is as follows: the two single

samples were laid flat and then stirred for 2 mins to ensure a uniform mixture. The sample is placed in the experimental sample cup and naturally compacted with weight. An S450 grating-type NIR spectrometer (Shanghai Lengguang Technology Ltd., China) was used to obtain the spectra of all samples. The spectra were collected between the wavelengths of 1000–2500 nm, with a resolution of 8 nm at the diffuse reflection mode. Data collected were in absorbance and were obtained by scanning for 90 s. The single and mixed samples were resampled three times each, three NIR spectral data were measured, and the average spectrum was considered to be the final spectrum.

TMS is calculated by the linear addition of single sample spectra according to the mixing percentage. In the legend, the simulated mixture spectra are suffixed with the suffix "simulated spectrum" after the name of the sample group. The actual mixture spectrum is added with the suffix "actual spectrum" after the name of the sample group.

2.3. Experimental Method

2.3.1. Simulated Mixture Spectrum. In this study, the simulated mixture spectrum, is obtained by the linear addition of the spectra of each single sample in the mixture according to their respective percentages. The formula is as follows:

$$\text{simulated mixture spectrum} = x_1 \times n_1\% + x_2 \times n_2\% + \cdots + x_i \times n_i\%.$$

(1)

where i denotes the ith single material, $x_1, x_2, \ldots, x_i$ denote the spectral data measured corresponding to the ith single material, $n_1\%, n_2\%, \cdots, n_i\%$ is the mass percentage corresponding to the ith single material in the mixture. For example, VB + VC(1)−simulated spectrum = VB spectral data×50% + VC spectral data × 50%.

2.3.2. Class of Constrained Regression (Formulation Regression). In this study, the formulation regression algorithm is used to analyze the percentages of the components of a mixture. This algorithm, which was proposed by the famous Chinese mathematician Kai-Tai Fang, is a regression algorithm with non-negative regression coefficients of sum (1). This method has been applied in the tobacco industry [31, 32], and its algorithmic model is described as follows [33, 34]:

$$\text{PR:} \begin{cases} Y = X\beta + \varepsilon\,(4a), \\ I_p'\beta = 1, \\ \beta \geq 0. \end{cases}$$

(2)

In the aforementioned PR model, Y is a $n \times 1$ matrix, X is a $n \times p$ $(n \geq p)$ matrix, β is a $p \times 1$ matrix, ε is a $n \times 1$ matrix, and I_p is a matrix with all 1 s in the data. Under the constraints of (1b) (1c), the least squares can be used to estimate β as follows:

$$Q = (Y - X\beta)^T (Y - X\beta) \longrightarrow \min.$$

(3)

TABLE 1: Particle size range of each component in the vitamin mixture.

Sample	Vitamin B$_3$ particle size (μm)	Vitamin C particle size (μm)
VB + VC (1)	<180	<180
VB + VC (2)	180–280	180–280
VB + VC (3)	280–450	280–450
VB + VC (4)	450–900	450–900
VB + VC (5)	<180	180–280
VB + VC (6)	<180	280–450
VB + VC (7)	280–450	450–900
VB + VC (8)	450–900	>900

TABLE 2: Mass percentages of japonica sorghum and glutinous sorghum in mixture samples.

Sample	Sorghum1	Sorghum2	Sorghum3	Sorghum4	Sorghum5
Mass percentage (%)	10–90	90–10	30–70	70–30	50–50

If $\beta^* \geq 0$ is obtained, the solution with the smallest β^* matrix is the unique solution of the PR model. Otherwise, the elimination change method is used to ensure the components of β^* remain non-negative.

In this study, independent variable Y constitutes the mixed sample spectral data vector, and the dependent variable X constitutes a single samples spectral data matrix. The percent vector β^*, which is solved according to the non-negative linear regression algorithm, is composed of the percentage coefficients, which can be used for quantitative analysis. For the binary quantitative analysis, two percentage coefficients exist. The sum of the two coefficients is 1, and the actual percentage coefficient is set as the criterion for accuracy.

2.3.3. Relative Deviation of the Spectrum. In this study, the difference between the actual mixed spectra and the simulated mixed spectra is detailed by comparing the relative deviation between the two spectra and whether the F and T tests pass. Here, the relative deviation is defined as follows:

$$RD\ (\%) = \frac{\sum_{i=1}^{n} |y_i - \widehat{y}_i|}{\sum_{i=1}^{n} |y_i|} \times 100. \tag{4}$$

where n is the number of spectral wavelength points, $y_1, y_2, \ldots, y_i$ are the actual spectral data, and $\widehat{y}_1, \widehat{y}_2, \ldots, \widehat{y}_i$ are the simulated spectral data. These data were measured by NIR diffuse reflectance. The basic assumption of this method is that the relative deviation is small when the actual mixed spectra coincide with the simulated mixed spectra. Thus, the particle size range of this sample group satisfies linear additivity.

3. Results and Discussion

3.1. Analysis of Small Differences in the Particle Size Range. Two starch-containing vitamin samples of the same particle size were prepared according to the procedure presented in Table 1.

The single sample spectra, the actual mixed spectra, and the corresponding simulated mixed spectra of samples VB + VC (1) –VB + VC (4) are displayed in Figure 1.

The "VB + VC (1)-simulated spectrum" and "VB + VC (1)-actual spectrum" of 1750–1850 nm in Figure 1(a) are enlarged in Figure 2.

The *F*-value, the *T*-value, and relative deviation between the actual mixed spectra and the simulated mixed spectra of the vitamin samples VB + VC (1)−VB + VC (4) are presented in Table 3.

The actual percentages, the analytic percentages, and the error between them of the vitamin samples VB + VC (1) –VB + VC (4) are presented in Table 4.

Figures 1(a)–1(b) and Figure 2 reveal that when the wavelength is in the range 1750–1850 nm, it belongs to the scattering region. No absorption of chemical groups is observed, which is defined as the chemically invalid absorption band. Analyzing the full spectrum affects the calculation accuracy. Therefore, the wavelengths in 1000–1749 nm and 1851–2500 nm were considered to be the characteristic bands. The scattering area becomes smaller as the particle size of the mixed sample expands, which effectively reduces the effect of scattering, as displayed in figures 1(c)–1(d).

In Figure 1 and Table 3, the actual mixed spectra and the corresponding simulated mixed spectra are highly consistent. No significant difference was observed between them at $\alpha = 0.01$, and the relative deviations are small, all within 1.03%. Table 4 reveals that the percentage of each component in the mixture analyzed by formula regression is close to the actual mixing mass ratio. The absolute error between the analytic percentage and the actual percentage is within 2.98%. Thus, the simulated mixed spectra obtained according to the linear addition principle in the range of less than 180, 180–280, 280–450, and 450–900 μm are consistent with the actual situation. The additivity of the diffuse reflectance spectra is feasible in the aforementioned range.

3.2. Analysis of the Expanded Particle Size Range. To determine the NIR diffuse reflectance linear additivity and gradually expand the range of mixed sample particle sizes, the sample sets of vitamin mixtures with various particle sizes are prepared according to Table 1.
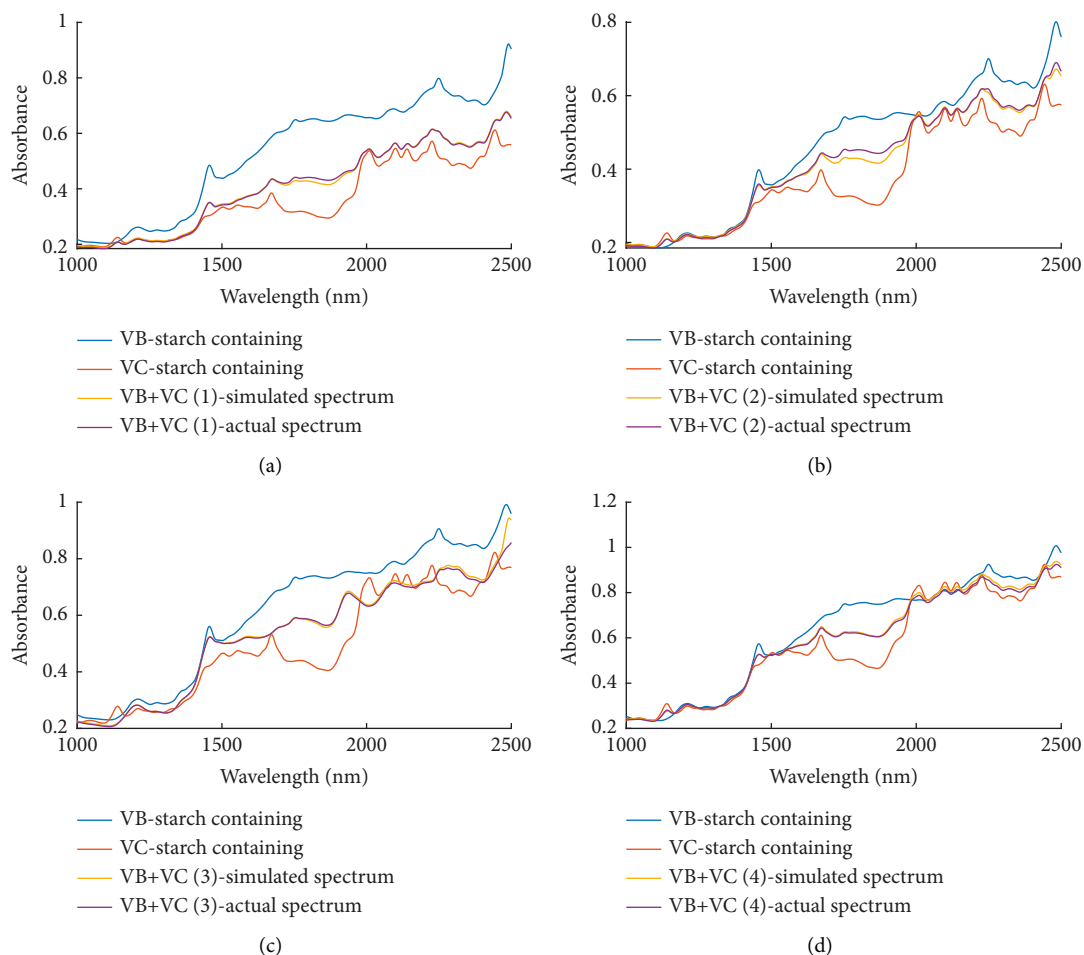
(a)

(b)

(c)

(d)

Figure 1: Single sample spectra, the actual mixed spectra, and the corresponding simulated mixed spectra of (a) samples VB + VC (1)−(<180 μm + <180 μm). (b) Samples VB + VC (2)−(180–280 μm + 180–280 μm). (c) Samples VB + VC (3)−(280–450 μm + 280–450 μm). (d) Samples VB + VC (4)−(450–900 μm + 450–900 μm).
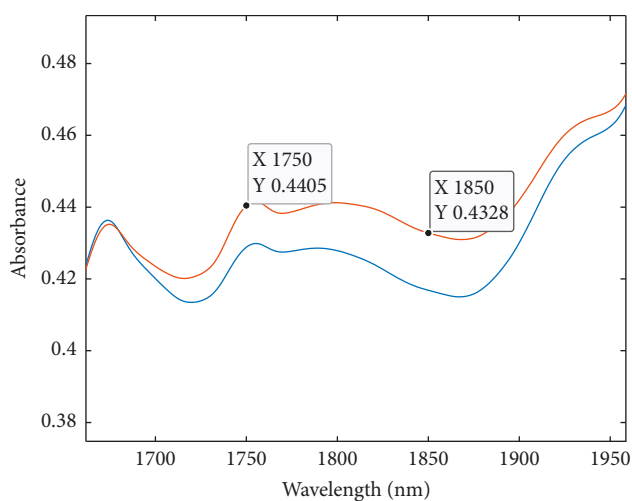

Figure 2: The "VB + VC (1)−simulated spectrum" and "VB + VC (1)−actual spectrum" of 1750–1850 nm.

The single sample spectra, the actual mixed spectra, and its corresponding simulated mixed spectra of the vitamin samples VB + VC (5)−VB + VC (8) are displayed in Figure 3.

Table 3: RD, F-value, and T-value between the actual mixed spectra and simulated mixed spectra of the vitamin samples VB + VC (1)−VB + VC (4).

|	F-value	T-value	RD of spectrum (%)
VB + VC (1)	1.0117	0.1871	0.82
VB + VC (2)	0.9690	0.2634	0.88
VB + VC (3)	0.6949	0.5490	0.81
VB + VC (4)	0.9569	0.6857	1.03
Threshold value	1.1277	2.3276	

The F-value, T values, and the relative deviation between the actual mixed spectra and the simulated mixed spectra of the vitamin samples VB + VC (5)−VB + VC (8) are presented in Table 5.

The actual percentages, the analytic percentages, and error between them of the vitamin samples VB + VC (5)−VB + VC (8) are presented in Table 6.

Figure 3, Table 5, and Table 6 reveal that as the particle size range of the sample group is expanded, the spectrograms and the corresponding data analysis of the sample group VB + VC (5) are in accordance with the diffuse reflection linear additivity. However, the actual

TABLE 4: Analytic percentage, actual percentage, and the error between them of the vitamin samples VB + VC (1)–VB + VC (4).

	Actual percentage (/%)	Analytic percentage (/%)	Absolute error (/%)
VB + VC (1)	50–50	51–49	1.04
VB + VC (2)	50–50	50–50	0.19
VB + VC (3)	50–50	49–51	−0.52
VB + VC (4)	50–50	53–47	2.98
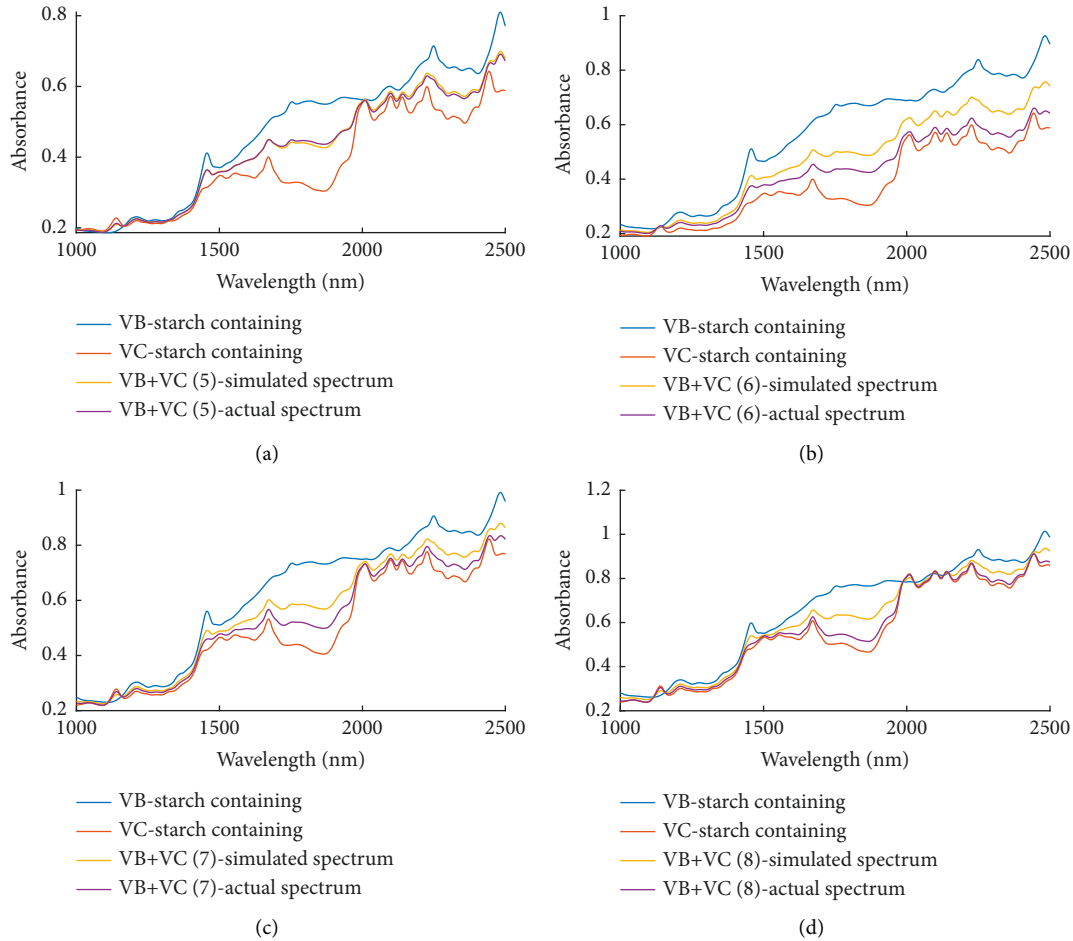
FIGURE 3: Single sample spectra, the actual mixed spectra, and the corresponding simulated mixed spectra of (a) sample VB + VC (5)−(<180 μm + 180–280 μm) (b) sample VB + VC (6)−(<180 μm + 280–450 μm) (c) sample VB + VC (7)−(280–450 μm + 450–900 μm) (d) sample VB + VC (8)−(450–900 μm+>900 μm).

TABLE 5: RD, F-value, and T-value of actual mixed spectra and simulated mixed spectra of the vitamin samples VB + VC (5)–VB + VC (8).

	F-value	T-value	RD of spectrum (/%)
VB + VC (5)	1.0244	0.3863	1.08
VB + VC (6)	1.0429	8.1721	11.14
VB + VC (7)	0.9322	3.1236	4.44
VB + VC (8)	0.9462	3.8294	5.41
Threshold value	1.1277	2.3276	

mixed spectra of VB + VC (6), VB + VC (7), and VB + VC (8) the sample groups differed significantly from the constructed simulated mixed spectra with large relative deviations, and the T-test failed. Thus, the scattering

coefficients varied considerably in this particle size range, and the diffuse reflectance spectra were not additive. Combining the sample groups under the same particle size, we have the following: the linear additivity can be satisfied when the particle size is in the range of <280 μm, 280–450 μm, and 450–900 μm.

3.3. Diffuse Reflectance Additivity of Sorghum Samples. To verify the aforementioned findings, five samples of japonica sorghum and glutinous sorghum with various gradient mass ratios were prepared according to Table 2.

The single sample spectra, actual mixed spectra, and corresponding simulated mixed spectra of sorghum samples are displayed in Figure 4.

TABLE 6: Analytic percentage, actual percentage, and absolute error between them of the vitamin samples VB + VC (5)−VB + VC (8).

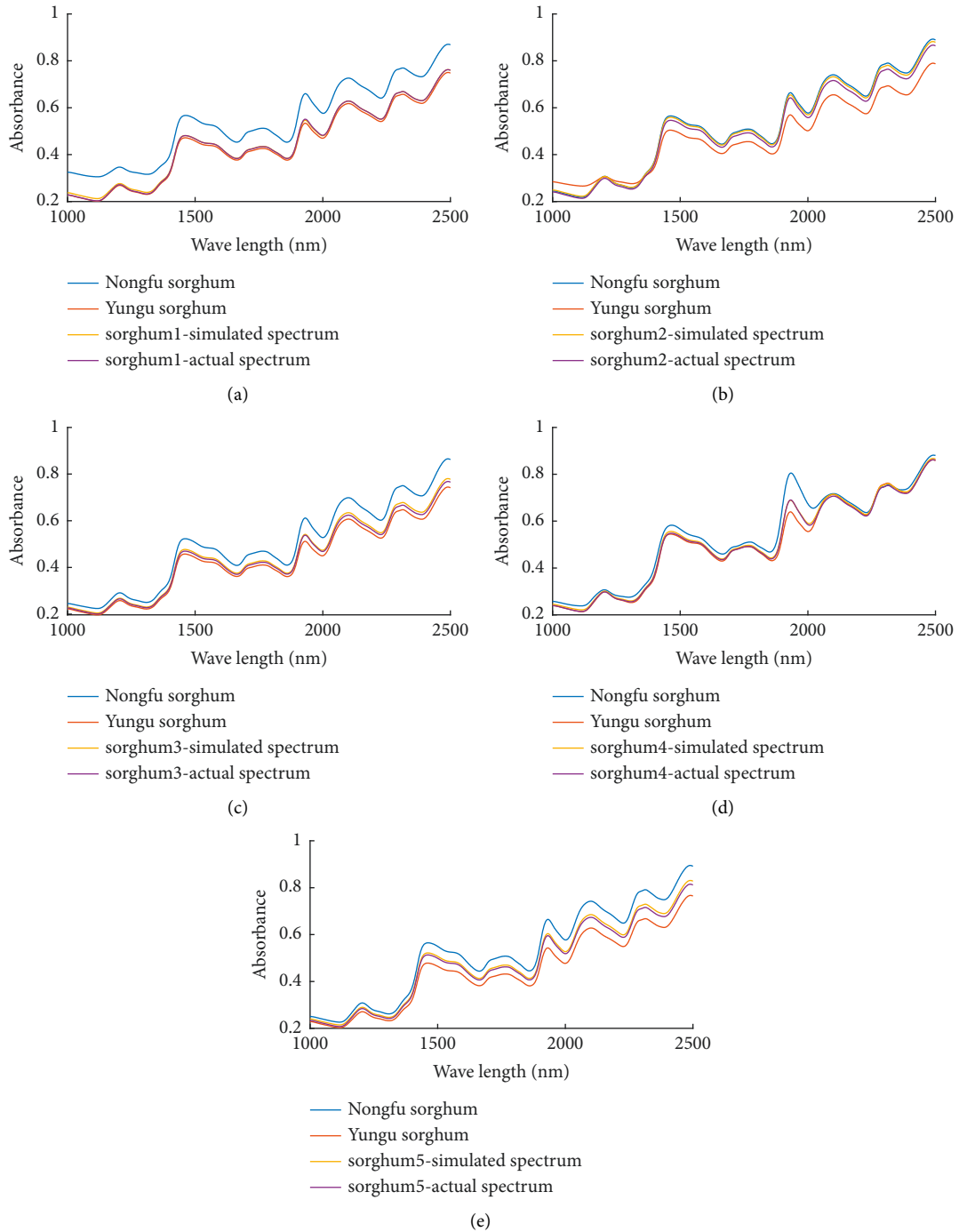|	Actual percentage (%)	Analytic percentage (%)	Absolute error (/%)
VB + VC (5)	50−50	52−48	2.28
VB + VC (6)	50−50	64−36	14.39
VB + VC (7)	50−50	30−70	-20.13
VB + VC (8)	50−50	84−16	34.08

(a)

(b)

(c)

(d)

(e)

FIGURE 4: Single sample spectra, actual mixed spectra, and the corresponding simulated mixed spectra of (a)sample group Sorghum1 (10%−90%), (b) sample group Sorghum2 (90%−10%), (c) sample group Sorghum3 (30%−70%), (d) sample group Sorghum4 (70%−30%), and (e) sample group Sorghum5 (50%−50%).

TABLE 7: RD of spectrum, F-value, and T-value of the actual mixed spectra and simulated mixed spectra of sorghum samples.

	F-value	T-value	RD of spectrum (/%)
Sorghum1	1.0298	0.4793	0.52
Sorghum2	0.9916	0.6309	0.35
Sorghum3	1.0220	0.2076	0.84
Sorghum4	1.0354	0.3116	0.51
Sorghum5	1.0226	0.2250	0.78
Threshold value	1.1277	2.3276	

TABLE 8: Analytic percentage, actual percentage, and the absolute error between them of sorghum samples.

	Actual percentage (%)	Analytic percentage (%)	Absolute error (/%)
Sorghum1	10–90	8–92	−1.92
Sorghum2	90–10	92–8	2.28
Sorghum3	30–70	3–70	0.62
Sorghum4	70–30	70–30	−0.30
Sorghum5	50–50	54–46	4.16

The F-value, T-values, and relative deviation between the actual mixed spectra and the simulated mixed spectra of sorghum samples are presented in Table 7.

The actual percentages, the analytic percentages, and the error between them of sorghum samples are presented in Table 8.

As displayed in Figure 4, Table 7, and Table 8, the actual mixed spectra and the simulated mixed spectra overlap considerably with insignificant differences and relative deviations less than 0.84%. Thus, they passed the F-test and T-test. The absolute error between actual and analytic percentage were within 4.16% when the powder particle size was in the range 280–450 μm. Thus, the linear additivity of NIR diffuse reflectance is feasible at various mass gradients.

3.4. Application of the Determination of Mixing Uniformity.
In case the percentage of each component in the mixture is known, the homogeneity of a material mixture can be detected when the material particle size range satisfies the NIR diffuse reflectance linear addition conditions. Two discrimination methods are listed as follows:

(i) The percentage of each component in the sample can be analyzed using the known complex material system spectra combined with the formulation regression algorithm. The error in the homogeneity of the material mixture was determined from the analytic percentage and the actual percentage. In medical research, researchers determine the homogeneity of a mixture by measuring the amount of a component in the mixture (comparing the percentages in the formulations) [35]. The principle of this method is similar to the determination method proposed in this study.

(ii) The NIR diffuse reflectance spectra of complex material systems are in accordance with the additive property of the spectral absorption values in that premise. The spectra of each component are added in corresponding percentages to produce a simulated mixed homogeneous spectrum. This spectrum is calculated as shown in equation (4). This spectrum represents the state in which the blend is uniformly mixed. F-test and T-test were applied to determine whether there is a significant difference between this spectrum and the actual mixture spectrum to evaluate the homogeneity of the mixture.

The flowchart for determining the mixing uniformity is displayed in Figure 5.

3.5. Application of Percentage Analysis.
When the mixture is known to be homogeneous, a formulation regression algorithm is used to analyze the percentages of the components. In textiles, the content of cotton, polyester, polyamide fibers, and other fabrics is required to be estimated in blended fabrics. In petrochemicals, the composition of gasoline blending components, such as olefins and octane values, vary considerably. Therefore, the percentages of various gasoline blending components can be analyzed.

The flowchart of the percent analysis is displayed in Figure 6.

3.6. Standard Normal Variate Spectrum.
The data for the vitamin and sorghum samples pretreated after standard normal variate (SNV) are presented in Tables 9 and 10, respectively. The table includes the analytic percentage, the actual percentage, the absolute error of both, the relative deviation between the actual mixed homogeneous spectrum, and the simulated mixed spectrum.

To eliminate the effect of uneven particle size and particle distribution on the measured spectrum, in this study, an SNV transformation preprocessing method was applied to verify whether the linear addition range can be extended. However, Table 9 reveals that the SNV pretreatment increases the relative deviation between the simulated mixed spectra and the actual mixed homogeneous spectra. The absolute error between the analytic and actual ratios also
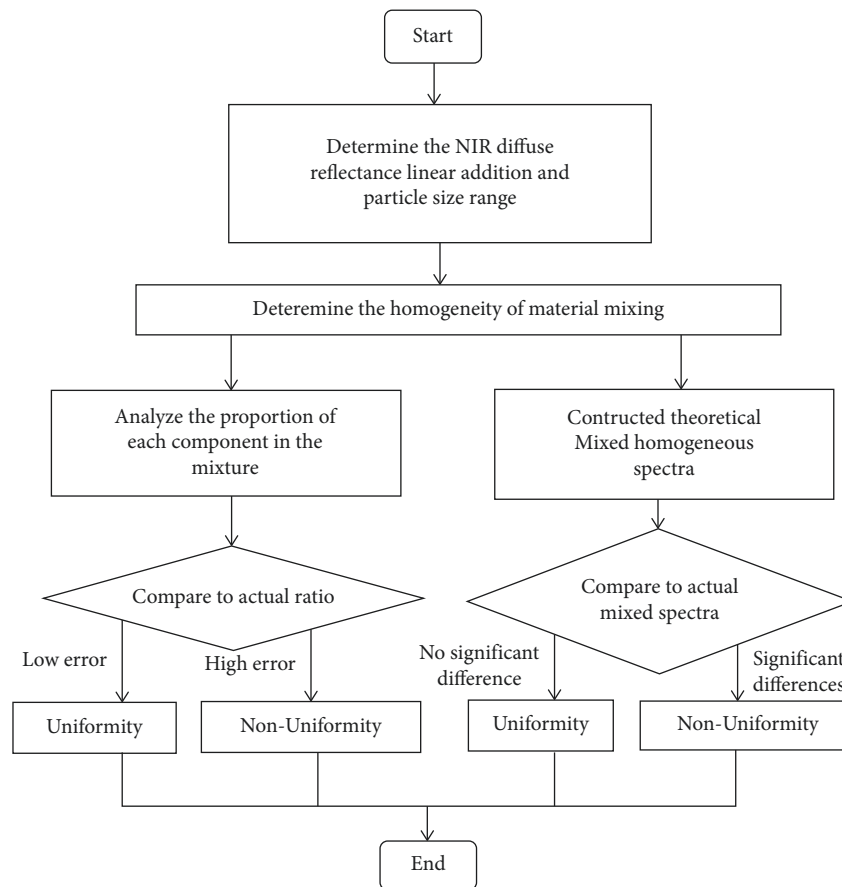
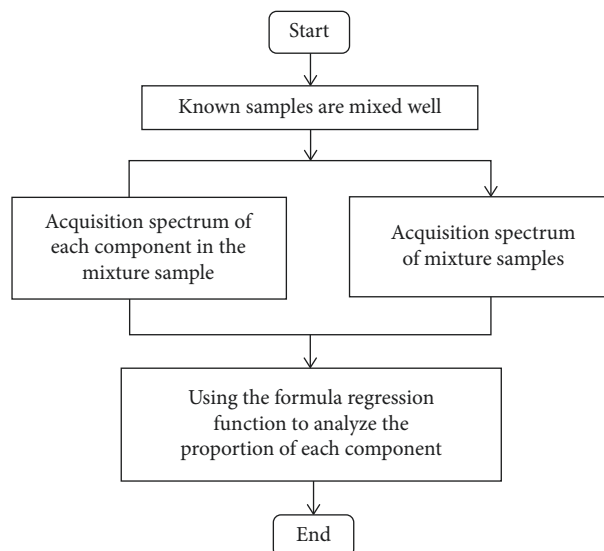FIGURE 5: Mixing uniformity determination flowchart.

FIGURE 6: Flow chart for analyzing the percentage of each component in the mixture.

increases considerably. Even in the homogeneous state of the mixture, these differences were aggravated by the pretreatment for the SNV-processed sample groups. Therefore, the range of near-infrared diffuse reflectance linear addition and use was still within the range of <280 μm, 280–450 μm, and 450–900 μm.

However, Table 10 reveals that for the sorghum samples, SNV pretreatment reduced the absolute error in the actual and analytic percentages. The relative deviation between the simulated mixed spectra and the actual mixed homogeneous spectra also reduced. SNV can effectively eliminate the effect of scattering on the spectra in sorghum sample measurements.

TABLE 9: The analytic percentage, the actual percentage, the absolute error of both, the relative deviation between the actual mixed homogeneous spectrum, and the simulated mixed spectrum of the vitamin sample.

Sample	Actual percentage (%)	Analytic percentage (%)	Absolute error (/%)	RD of spectrum (/%)
VBC1	50–50	46–54	−3.59	2.11
VBC2	50–50	46–54	−4.44	2.45
VBC3	50–50	54–46	3.84	2.57
VBC4	50–50	50–50	0.40	0.97
VBC5	50–50	52–48	2.34	2.22
VBC6	50–50	73–27	23.32	5.05
VBC7	50–50	30–69	−19.16	8.86
VBC8	50–50	83–17	32.82	12.58

TABLE 10: The analytic percentage, the actual percentage, the absolute error of both, the relative deviation between the actual mixed homogeneous spectrum, and the simulated mixed spectrum for sorghum samples.

Sample	Actual percentage	Analytic percentage	Absolute error (/%)	RD of spectrum (/%)
Sorghum1	10–90	8–92	−1.60	0.52
Sorghum2	90–10	92–8	1.92	0.49
Sorghum3	30–70	30–70	0.20	0.57
Sorghum4	70–30	76–24	5.86	0.84
Sorghum5	50–50	51–48	1.71	0.72

4. Conclusion

This study revealed that the particle size range of $<280\,\mu m$, $280–450\,\mu m$, and $450–900\,\mu m$ satisfies the condition of linear addition. On this basis, we propose the use of NIR analysis technique to determine the homogeneity of material mixing. By building a mechanical model, a discriminative analysis of the material mixing situation can be achieved. As a simple and fast method to identify medicine and design agricultural product formulations, the method has a broad application prospect. The linear addition based on spectra and direct calibration approach and the percentages of the components in a mixture can be analyzed. It does not need to use a large amount of data to build statistical models. This method only requires the use of a single spectrum of each component of the mixture and a mixture spectrum.

However, the SNV pretreatment method was not effective. Therefore, further research on spectral pretreatment method is critical for reducing the scattering effect. The range of particle sizes that satisfy the linear addition property should be expanded. The materials used in this study exhibit similar density. Therefore, the mass percentage is used in the experiments. For samples with large density differences, further verification is still required.

Data Availability

The spectral data used to support the findings of this study are included within the supplementary materials.

Conflicts of Interest

The authors declare that there are no potential conflicts of interest with respect to the research, authorship, and/or publication of this article.

Acknowledgments

Supplementary Materials

The supplementary material contains the spectral data that was used to support the findings of the manuscript. In the data file, column A gives sample group, column B gives sample's name, and the other columns show the spectral data. The first row presents the wavenumber value. (*Supplementary Materials*)

References

[1] É. Szabó, S. Gergely, T. Spaits, T. Simon, and A. Salgó, "Near-infrared spectroscopy-based methods for quantitative determination of active pharmaceutical ingredient in transdermal gel formulations," *Spectroscopy Letters*, vol. 52, no. 10, pp. 599–611, 2019.

[2] T. Woodcock, G. Downey, and C. P. O'Donnell, "Better quality food and beverages: the role of near infrared spectroscopy," *Journal of Near Infrared Spectroscopy*, vol. 16, no. 1, pp. 1–29, 2008.

[3] J. Lin, L. Yu, W. Li, and H. Qin, "Method for identifying maize haploid seeds by applying diffuse transmission near-infrared spectroscopy," *Applied Spectroscopy*, vol. 72, no. 4, pp. 611–617, 2018.

[4] H. Cen and Y. He, "Theory and application of near infrared reflectance spectroscopy in determination of food quality," *Trends in Food Science & Technology*, vol. 18, no. 2, pp. 72–83, 2007.

[5] L. Yin, J. Zhou, D. Chen et al., "A review of the application of near-infrared spectroscopy to rare traditional Chinese medicine," *Spectrochimica Acta Part A: Molecular and Biomolecular Spectroscopy*, vol. 221, Article ID 117208, 2019.

[6] W.-Q. Yao, D.-L. WU, Y.-M. WU, and M.-X. Peng, "Comparison of mid-infrared analysis model and near-infrared analysis model of nicotinamide in multi-vitamin B," *Chemical Reagents*, vol. 42, no. 10, pp. 1190–1195, 2020.

[7] J. E. Lewis, E. Tiozzo, A. B. Melillo et al., "The effect of methylated vitamin b complex on depressive and anxiety symptoms and quality of life in adults with depression," *ISRN Psychiatry*, vol. 2013, Article ID 621453, 7 pages, 2013.

[8] K. Xu, R. Peng, Y. Zou, X. Jiang, Q. Sun, and C. Song, "Vitamin C intake and multiple health outcomes: an umbrella review of systematic reviews and meta-analyses," *International Journal of Food Sciences & Nutrition*, vol. 73, no. 5, pp. 588–599, 2022.

[9] B. R. A. Junior, F. L. F. Soares, J. A. Ardila, L. G. C. Durango, M. R. Forim, and R. L. Carneiro, "Determination of B-complex vitamins in pharmaceutical formulations by surface-enhanced Raman spectroscopy," *Spectrochimica Acta Part A: Molecular and Biomolecular Spectroscopy*, vol. 188, pp. 589–595, 2018.

[10] D. H. Rhodes, L. Hoffmann, W. L. Rooney et al., "Genetic architecture of kernel composition in global sorghum germplasm," *BMC Genomics*, vol. 18, no. 1, p. 15, 2017.

[11] Y. Tang, "Study on the technical parameters of liquor-making from glutinous sorghum and non-glutinous sorghum," *Liquor-making Science & Technology*, vol. 21, no. 6, pp. 44–46, 2000.

[12] M. Tang and X. Cheng, "Application of sorghum in feed," *China Feed*, vol. 24, no. 4, pp. 39–41, 2013.

[13] V. Mizonov, I. Balagurov, H. Berthiaux, and C. Gatumel, "Intensification of vibration mixing of particulate solids by means of multi-layer loading of components," *Advanced Powder Technology*, vol. 28, no. 11, pp. 3049–3055, 2017.

[14] M. Yamamoto, S. Ishihara, and J. Kano, "Evaluation of particle density effect for mixing behavior in a rotating drum mixer by DEM simulation," *Advanced Powder Technology*, vol. 27, no. 3, pp. 864–870, 2016.

[15] J. G. Rosas and M. Blanco, "A criterion for assessing homogeneity distribution in hyperspectral images. Part 1: homogeneity index bases and blending processes," *Journal of Pharmaceutical and Biomedical Analysis*, vol. 70, pp. 680–690, 2012.

[16] S. Krukowski, M. Karasiewicz, and W. Kolodziejski, "Convenient uv-spectrophotometric determination of citrates in aqueous solutions with applications in the pharmaceutical analysis of oral electrolyte formulations," *Journal of Food and Drug Analysis*, vol. 25, no. 3, pp. 717–722, 2017.

[17] S. Görög, *Ultraviolet-visible Spectrophotometry in Pharmaceutical Analysis*, CRC Press, Boca Raton, Florida, 2018.

[18] C. Yin, H. Lei, C. Xingning et al., "Study on mixed prediction model of nitrate concentration in water based on ultraviolet spectroscopy," *Spectroscopy and Spectral Analysis*, vol. 39, no. 5, pp. 1489–1494, 2019.

[19] G. Léonard, F. Bertrand, J. Chaouki, and P. M. Gosselin, "An experimental investigation of effusivity as an indicator of powder blend uniformity," *Powder Technology*, vol. 181, no. 2, pp. 149–159, 2008.

[20] A. S. El-Hagrasy, H. R. Morris, F. D'amico, R. A. Lodder, and J. K. Drennen, "Near-infrared spectroscopy and imaging for the monitoring of powder blend homogeneity," *Journal of Pharmaceutical Sciences*, vol. 90, no. 9, pp. 1298–1307, 2001.

[21] B. Ma, M. Wang, D. Tian, Y. Pei, and L. Yuan, "Micro/nano-structured polyaniline/silver catalyzed borohydride reduction of 4-nitrophenol," *RSC Advances*, vol. 5, no. 52, pp. 41639–41645, 2015.

[22] S. O. Eraga, M. I. Arhewoh, R. N. Chibuogwu, and M. A. Iwuagwu, "A comparative UV-HPLC analysis of ten brands of ibuprofen tablets," *Asian Pacific Journal of Tropical Biomedicine*, vol. 5, no. 10, pp. 880–884, 2015.

[23] C. Hua long and L. Wang pei, "Determination of content and content uniformity of vitamin B_1, vitamin B_2 and niacinamide in compound vitamin B tablets by HPLC," *Strait Pharmaceutical Journal*, vol. 28, no. 2, pp. 63–65, 2016.

[24] J. Fiori, G. Grassigli, P. Filippi, R. Gotti, and V. Cavrini, "HPLC-DAD and LC-ESI-MS analysis of doxycycline and related impurities in doxipan mix, a medicated premix for incorporation in medicated feedstuff," *Journal of Pharmaceutical and Biomedical Analysis*, vol. 37, no. 5, pp. 979–985, 2005.

[25] E. Bharvada, V. Shah, and M. Misra, "Exploring mixing uniformity of a pharmaceutical blend in a high shear mixture granulator using enthalpy values obtained from DSC," *Powder Technology*, vol. 276, pp. 103–111, 2015.

[26] Y. Takeuchi, M. Yoshida, A. Ito, and H. Sunada, "Uniformity of drug content during pharmaceutical dry granulating by roller compaction and tableting processes," *Journal of Drug Delivery Science and Technology*, vol. 19, no. 2, pp. 119–124, 2009.

[27] Y. Sulub, M. Konigsberger, and J. Cheney, "Blend uniformity end-point determination using near-infrared spectroscopy and multivariate calibration," *Journal of Pharmaceutical and Biomedical Analysis*, vol. 55, no. 3, pp. 429–434, 2011.

[28] A. Barone, J. Glassey, and G. Montague, "Towards online near-infrared spectroscopy to optimise food product mixing," *Journal of Food Engineering*, vol. 263, pp. 227–236, 2019.

[29] W. Momose, K. Imai, S. Yokota, E. Yonemochi, and K. Terada, "Process analytical technology applied for end-point detection of pharmaceutical blending by combining two calibration-free methods: simultaneously monitoring specific near-infrared peak intensity and moving block standard deviation," *Powder Technology*, vol. 210, no. 2, pp. 122–131, 2011.

[30] Y. Yan, L. Zhang, J. Mao, and G. Yan, "Studies on the theoretic bases of applied FTNIRDRSA," *Journal of China Agricultural University*, vol. 36, no. S2, pp. 5–17, 1990.

[31] X. Li, R. Shu, L. Lili et al., "Study on the analysis of the percentage of mixed samples with near infrared spectroscopy and non-negative coefficients regression," *Spectroscopy and Spectral Analysis*, vol. 36, no. 4, pp. 967–971, 2016.

[32] J. Liu, J. Hu, F. Yang, and G. H. Y. Panpan, "Detection of mixing percentage of stem by near infrared Spectroscopy combined with linear non-negative regression coefficient regression method," *Food&Machinery*, vol. 37, no. 11, pp. 188–192, 2021.

[33] F. Kai-tai, D.-q. Wang, and W. Guo-fu, "A class of constrainted regression-programing regression [J]," *Mathematica Numerica Sinica*, vol. 4, no. 1, pp. 57–69, 1982.

[34] F. Kai-tai and S.-D. He, "Regression models with linear constraints and nonnegative regression coefficients," *Mathematica Numerica Sinica*, vol. 7, no. 3, pp. 237–246, 1985.

[35] M. Popo, S. Romero-Torres, C. Conde, and R. J. Romañach, "Blend uniformity analysis using stream sampling and near infrared spectroscopy," *AAPS PharmSciTech*, vol. 3, no. 3, pp. 61–71, 2002.